Comparison of N×2D and 3D Split-Step Fourier Methods in Realistic 3D Ducting Conditions

Hang Zhou[(1)(2)], Rémi Douvenot[(1)(2)], and Alexandre Chabory[(1)(2)]
(1) ENAC, TELECOM-EMA, F-31055 Toulouse, France
(2) Toulouse University, F-31400 Toulouse, France
Email: hang.zhou@recherch.enac.fr, alexandre.chabory@recherche.enac.fr

***Abstract*—A 3D split-step Fourier method is presented and tested. It is based on a spectral representation of the discrete wave equation in cylindrical coordinates. The formulations in this method are self-consistent in the discrete domain. This method is applied to simulate the propagation with ducts retrieved after clutter data inversion. In the numerical tests, the difference between N × 2D and 3D models is not significant. Thus, in this case, considering the 3D atmosphere effects is unnecessary.**

Keywords—3D propagation; discrete formulation; troposphere propagation; ducts

I. INTRODUCTION

The split-step Fourier method is widely used to simulate the wave propagation in 2D vertical planes [1]. To model a 3D scene, a N × 2D model approximation scanning all azimuth angles is classically used. However, N×2D models neglect lateral effects. These latter appear in the case of irregular reliefs and/or non-constant refractive index.

Accurate 3D models are required for the wave propagation in complex environments. A 3D split-step Fourier method based on a spectral representation of the discrete wave equation in cylindrical coordinates has been proposed by Zhou et al. [2]. This formulation is self-consistent in the discrete domain. Obtained in cylindrical coordinates, this method is also more suitable for radar propagation than those in Cartesian coordinates. The method can handle a slowly varying inhomogeneous atmosphere using phase screens.

In this paper, this method is applied to a realistic 3D ducts. The ducts over the sea are obtained by inversion of clutter data measurements [3]. In the numerical test, both simulations using 3D and N×2D methods are compared.

II. CONFIGURATION

The cylindrical coordinate system (r,θ,z) is used. The sources are assumed inside the cylinder $r \leq r_0$ and the fields/potentials are known at $r = r_0$. A perfect metallic and infinite planar ground is located at $z = 0$. The propagation is computed in the region $r > r_0$, $z > 0$. The fields are represented by TE and TM components with respect to z by means of Hertz potentials. In this paper, only the TE component is considered. The TM component could be simulated in a similar way.

For numerical applications, the computation domain is discretized and of finite size. Thus, the vertical domain is limited to $z \in]0,z_{\max}[$ and the following uniform grid is used:

$$\begin{cases} r = p_r \Delta r \text{ for } p_r = \{1,\dots,N_r-1\}, \\ z = p_z \Delta z \text{ for } p_z = \{1,\dots,N_z-1\}, \\ \theta = p_\theta \Delta\theta \text{ for } p_\theta = \{0,\dots,N_\theta-1\}, \end{cases} \quad (1)$$

with $\Delta r = r_{\max}/N_r$, $\Delta z = z_{\max}/N_z$ and $\Delta\theta = 2\pi/N_\theta$.

III. 3D SPLIT-STEP FOURIER METHOD

The computation is performed marching on in distance. The potential Ψ on the cylinder at distance $r_0 + p_r\Delta r$ is expressed in the spectral domain by Fourier transforms. We propagate the potential through a homogeneous medium using the spectral propagator Λ, such that [2]

$$\Lambda_{p_r,q_\theta,q_z} = \frac{H_\kappa^{(2)}\left(k_r(r+\Delta r)\right)}{H_\kappa^{(2)}(k_r r)}\sqrt{\frac{r+\Delta r}{r}}, \quad (2)$$

with $r = r_0 + p_r\Delta r$, where

$$\kappa = \frac{2}{\Delta\theta}\sin\left(\frac{\pi q_\theta}{N_\theta}\right) \text{ for } q_\theta = \{0,\dots,N_\theta-1\}, \quad (3)$$

and $k_r^2 = k_0^2 n^2 - k_z^2$ with

$$k_z = \frac{2}{\Delta z}\sin\left(\frac{\pi q_z}{2N_z}\right) \text{ for } q_z = \{1,\dots,N_z-1\}. \quad (4)$$

Then the spectrum is expressed in the spatial domain with inverse Fourier transforms. This propagator differs from the one classically used [4], because it is obtained from a discretized wave equation.

In the spatial domain, we apply a phase screen to account for the refraction index variations. To remove reflections over the top boundary, an apodization is applied with a Hanning window on the top half area in the spatial domain. In the final step, the field is calculated from the potential.

IV. NUMERICAL TEST

A. Refractive index model

To highlight the 3D effects of the atmosphere, a refractive index model in the presence of a duct with azimuthal variations is required. Since we have no measured data of the refractive index with strong azimuthal variations, we choose the ducts retrieved after clutter data inversion by

Douvenot *et al.* [3]. In their work, measured clutter data with Spandar radar [5] of frequency 2.84GHz are inversed to infer the refractive index along a 90° azimuthal aperture. The retrieved ducts are plotted in Fig. 4. of [3]. We focus on the 24° azimuthal sector where the duct has the stronger azimuthal variation. The maximum gradients are 0.91 M-units/m in vertical and 0.98 M-units/deg in azimuth.

B. Configuration of the test

In the simulation, a 2D complex source point [6] at height 30.78 m is used with the same frequency as Spandar radar. The waist width of the source is chosen as 0.5 m. The center of the source is at azimuth 150°. The simulation parameters are $r_0 = 2$ km, $r_{max} = 60$ km, $\Delta r = 0.2$ m, $z_{max} = 204.8$ m, $\Delta z = 0.2$ m. The sectoral propagation method [2] is applied in a sector from 138° to 162° , discretized on $N_\theta = 10000$ points. The sea surface is modelled as a perfect electric conductor in the test.

C. Propagation test

The normalized electric field obtained at distance $r_{max} = 60$ km is shown in Fig. 1. Due to the atmosphere ducts over the sea, we can see a deformation of the final field. The difference between the normalized final fields obtained with the 3D and the N×2D models are shown in Fig. 2. The difference is negligible. The difference of the electric field normalized at each range on the horizontal plane at the height of the source between 3D and N×2D methods is shown in Fig. 3. The difference is also negligible.

The proposed 3D model is theoretically more accurate than the N×2D model. However, the difference here is not significant because the azimuthal gradient of refractivity is minor. N × 2D methods should be preferred, since 3D method is resource intensive. This simulation is performed on a standard desktop computer. The computation time of the 3D model is about 6 hours, and the one of N×2D model is about 1 hour ($N_\theta = 10000$).

V. Conclusion

An application of the 3D split-step Fourier method based on a spectral representation of the discretized wave equation in cylindrical coordinates has been presented with realistic ducting conditions. The ducts over a sea retrieved after clutter data inversion have been used. Both simulations using 3D and N × 2D methods have been performed to compare the difference. The 3D model has a better accuracy since lateral effects are considered. However, in ducting conditions, the azimuthal gradient is not significant. Hence, the use of N×2D methods to model this type of scenarios is justified.

References

[1] M. Levy, Parabolic Equation Methods for Electromagnetic Wave Propagation. IET, 2000, no. 45.

[2] H. Zhou, A. Chabory and R. Douvenot "A 3D Split-Step Fourier Algorithm Based on a Discrete Spectral Representation of the Propagation Equation", IEEE Trans. Antennas Propag., 2017, in press.

[3] R. Douvenot, V. Fabbro, "On the knowledge of radar coverage at sea using real time refractivity from clutter," in IET Radar, Sonar & Navigation, vol. 4, no. 2, pp. 293-301, April 2010.

[4] W. L. Siegmann, G. A. Kriegsmann, and D. Lee, "A wide-angle threedimensional parabolic wave equation," Journal of the Acoustical Society of America, vol. 78, no. 2, pp. 659–664, 1985.

[5] P. A. Ingwersen, W. Z. Lemnios. "Radars for ballistic missile defense research", Lincoln Laboratory Journal, 12(2): 245-266, 2000.

[6] G. A. Deschamps, "Gaussian beam as bundle of complex rays," Electronic Letters, vol. 7, no. 23, pp. 684-685, 1971

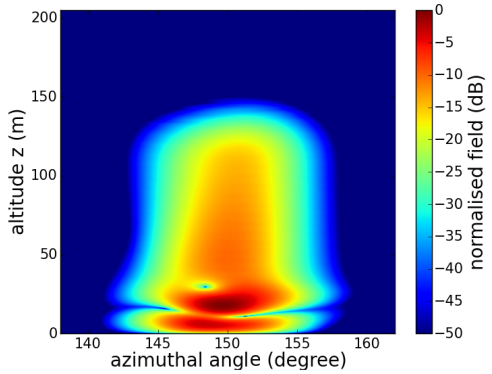

Fig. 1. Normalized final electric field (dB) using the proposed 3D method.

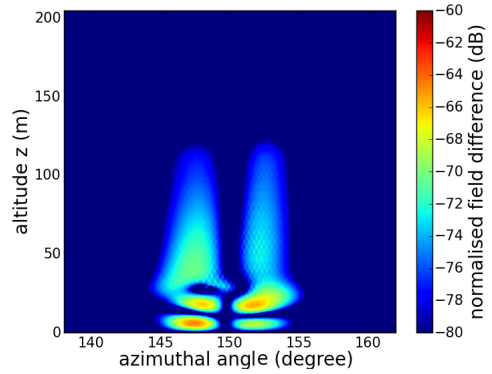

Fig. 2. Difference of normalized final electric fields (dB) between 3D and N×2D methods.

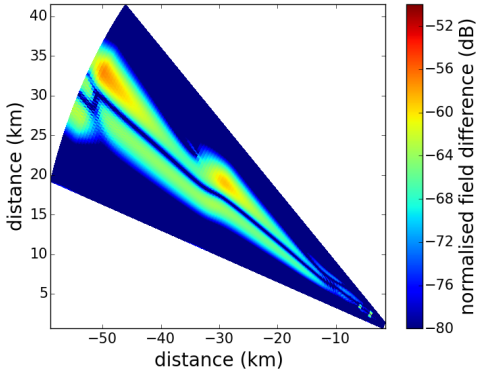

Fig. 3. Difference of normalized electric fields (dB) on the horizontal plane at height of the source between 3D and N×2D methods.